TRITONE: RF Insensitive T1 Estimator using SPGR acquisitions.

R. Fleysher[1], L. Fleysher[1], S. Liu[1], and O. Gonen[1]
[1]Radiology, NYU School of Medicine, New York, New York, United States

INTRODUCTION. Many studies have been devoted to developing T_1 measurement strategies based on several SPGR acquisitions that remain accurate even in the presence of the B_1 inhomogeneities encountered at fields above 3T (1,2). All, however, share several limitations: 1) the choice of acquisition parameters is restricted in one way or another; 2) the effects of the MR signal decay during the readout and, most important, 3) the restriction of total imaging time are ignored. While these self imposed restrictions sometimes simplify data analyses (1), they may also be deleterious to the precision of the derived T_1 maps (2), limiting their usefulness. Here, we optimize *all* parameters of three SPGR sequences without any restrictions (except field of view (FOV), resolution and total imaging time) to obtain accurate and precise T_1's. Owing to the SPGR-triplet-for-T_1 approach, we name this method TRITONE.

THEORY. In the SPGR sequence, the image intensity, S, is related to the apparent transverse relaxation time T_2^*, spin density, ρ_0, nominal flip angle (FA), α, transmit RF inhomogeneity described by the actual-to-nominal angle ratio (B_1), echo time, T_E, and repetition time, T_R, by Eq. [1].

$$S = \rho_0 \frac{1-e^{-T_R/T_1}}{1-e^{-T_R/T_1}\cos(B_1\alpha)} \sin(B_1\alpha) e^{-T_E/T_2^*} \quad [1]$$

$$\sigma_{T_1}^2 = \sigma_0^2(T_{adc})\left[\frac{1}{N_1}\left(\frac{\partial T_1}{\partial S_1}\right)^2 + \frac{1}{N_2}\left(\frac{\partial T_1}{\partial S_2}\right)^2 + \frac{1}{N_3}\left(\frac{\partial T_1}{\partial S_3}\right)^2\right] \quad [2]$$

Given three images S_1, S_2, S_3, obtained with different acquisition parameters, T_1 can be estimated from two ratios, say S_1/S_3 and S_2/S_3, numerically. If $\sigma_0(T_{adc}) \propto 1/\sqrt{T_{adc}}$ (3) is the standard deviation of the random noise in an individual image, determined by a common sample, instrument, readout duration, T_{adc} ($T_{adc} \leq 2T_E$), FOV and resolution then, using error propagation arguments (4), the variance σ_{T1} in T_1 (Eq. [2]) can be minimized in the vicinity of T_1^{tune} subject to the total imaging time constraint $T=N_1T_{R,1}+N_2T_{R,2}+N_3T_{R,3}$ where N_1, N_2 and N_3 are the number of averages of each acquisition in the triplet. Since 15% variations of B_1 around ideal B_1^{tune}=1.0 are common at 3T (5,6), instead of minimizing the error at B_1^{tune} we minimize the average at B_1^{tune}=0.85 and B_1^{tune}=1.15. Optimality of protocols requires T_{adc} be as close to T_2^* as possible (7). Once a protocol is chosen, Eq. [2] can be used to compute T_1 precision for any (T_1, B_1) pair as exemplified in Fig. 1 for $T=10T_1^{tune}$ protocol. Similar to two-SPGR measurements (7), the error drops faster than the square root of imaging time when *all* parameters are allowed to take more favorable values as permitted by the available time.

METHODS. Experiments were performed on a 3T Siemens Trio whole-body imager (Siemens AG, Erlangen, Germany) using its transmit-receive head coil, on a uniform 15cm diameter, 40cm length cylindrical water phantom of $T_1 \approx$ 300ms using a 64-shot 3D EPI SPGR with 192×192×96 mm^3 FOV and 64×64×32 matrix and *in vivo* in a human brain using a 224-shot 3D EPI SPGR with 224×224×64 mm^3 FOV and 224×224×64 matrix. The optimized protocol (T_R/T_1^{tune}, *FA, N* of the triplet are (2.2, 50, 1), (0.1, 50, 36), (4.2, 130, 1)) was tuned to T_1^{tune}=300ms for the phantom and T_1^{tune}=1000ms *in vivo* leading to experiments lasting 3.2 and 37.3 min respectively. The volunteer was briefed and gave institutional review board-approved written consent.

RESULTS. The width of the T_1 histogram of the phantom (Fig. 2) gauges the precision to a remarkable 1.8%. The 12.5% width of the *in vivo* white matter peak (Fig. 3) is very close to the 11% extrapolated from the phantom experiment by correcting for voxel volume and number of k-lines indicating that WM is very uniform in terms of T_1.

CONCLUSION. The normalized error ε_{T1} at T_1^{tune} of the DESPOT1 method (8,9) can not be smaller than 4.5 (7), and not smaller than 3.6 of its optimized version (7). TRITONE could achieve 4.2 (Fig. 1). Despite the complication caused by flip angle non-uniformity, TRITONE's precision is comparable to that of the two-SPGR methods (7,8,9) in the same time and spatial resolution and exceeds them in accuracy. If the two-SPGR methods are combined with B_1 measurement for accuracy, then TRITONE supersedes them in precision in the same total time.

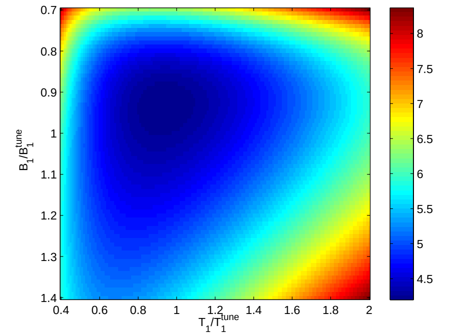

Fig.1 *Example of the normalized error* $\varepsilon_{T1} = (\sigma_{T1}/T_1)\sqrt{T}$ *as a function of* T_1 *and* B_1*. Note that the surface is very flat for a wide range of* T_1*'s and* B_1*'s. The minimal error is* ε_{T1}^{min}*=4.2.*

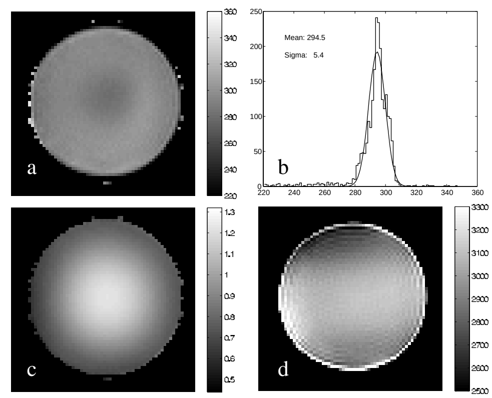

Fig. 2 a: *An axial* T_1 *map in a uniform phantom.* **b:** *Histogram of the* T_1 *values (jagged line) overlaid with the fitted Gaussian (solid line).* **c:** *The* B_1 *at the center and the edges is 20% above and below the nominal respectively.* **d:** B_1*-corrected* T_2^**-weighted spin density obtained using the reciprocity principle.*

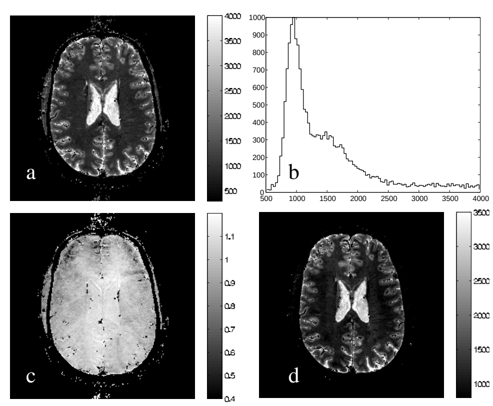

Fig. 3 a: *An axial* T_1 *map in a human brain at 1×1×1 mm*^{3}*.* **b:** *Histogram of the* T_1 *values exhibits a narrow WM peak at 950ms and broader GM at 1550ms.* **c:** *The* B_1 *at the center and the edges is 15% above and below the nominal respectively.* **d:** B_1*-corrected* T_2^**-weighted spin density obtained using the reciprocity principle. In all panels, black speckles represent pixels where signals could not be described by Eq. [1] presumably due to intravoxel variations of* T_1 *or motion.*

References. (1) Li T-Q., Deoni SC., Proc ISMRM 2006; 14:2643. (2) Mintzopoulos D., Inati S., Proc ISMRM 2006; 14:923. (3) Macovski A. Noise in MRI. Magn Reson Med 1996;36:494. (4) Bevington P. Data Reduction and Error Analysis for the Physical Sciences (Chapter 6). New York: McGraw-Hill; 1969. (5) Cheng H., Wright G., Magn Reson Med 2006;55:566-574. (6) Wang J., et al., Magn Reson Med 2005;53:408. (7) Fleysher L. et al., Magn Reson Med 2007;57:380. (8) Deoni SC, Rutt BK, Peters TM. Magn Reson Med 2003;49:515. (9) Wang HZ, Riederer SJ, Lee JN. Magn Reson Med 1987;5:399.